RADAR OBSERVATIONS OF OROGRAPHIC PRECIPITATION OVER COASTAL NORTHERN CALIFORNIA

Curtis N. James*
Embry-Riddle Aeronautical University, Prescott, Arizona

Robert A. Houze, Jr.
University of Washington, Seattle, Washington

1. INTRODUCTION

Coastal Northern California is an ideal laboratory for observing stable orographic precipitation. Deep convection is rare along the West Coast, and heavy precipitation is usually associated with land-falling baroclinic systems that direct strong, moist low-level flow against the terrain from the Pacific Ocean. During these events, heavy rainfall accumulation (up to 250 mm/day) can occur. The rain may combine with rapid snowmelt and produce extreme flooding of local rivers and streams.

The terrain in the region contains quasi two-dimensional mountain ridges that are analogous to traditional idealized model studies of flow over terrain. The ridges are oriented from north-northwest to south-southeast (Fig. 1) and are approximately orthogonal to the prevailing low-level flow during heavy precipitation events. The ridges known as the King Range and South Fork Mountain will be prominent in subsequent discussions of this paper.

This study explores the pattern of orographic precipitation enhancement over the coastal mountains of northern California and how the pattern relates to the strength and stability of the upstream flow. In this effort, WSR-88D radar data was collected over a 2.5-year period at Eureka, California (Fig. 1). The radar covers the precipitation both over the ocean and as it crosses the windward slopes of the mountain barrier. The radar echo climatology was analyzed in relation to the topography, wind, and thermodynamic stratification. This analysis elucidates orographic precipitation processes by analyzing not only the mean horizontal precipitation patterns but also the mean vertical structure of the radar echo in relation to the coastline and mountainous terrain.

2. DATA AND METHODS

The basic data set for this study is a 2.5-year archive of major precipitation events from the Eureka, California, WSR-88D (Fig. 1). The radar is located near Cape Mendocino and covers much of the precipitation both over the ocean and as it crosses the windward slopes of the mountain barrier. Radar data archives were available for 61 of the 67 heavy precipitation days during 1 October 1995 - 31 March 1998, a period including the CALJET and COAST experiments. A major precipitation event was defined as a day on which at least 25% of the 73 automated rain gauges in the region bounded by 39 °N, 42 °N, 122 °W, and the California coastline recorded 25 mm (1 in) or more of precipitation. The white circles in Fig. 1 show the locations of the gauges. The basic unit of radar data was the three-dimensional volume scanned by the WSR-88D elevation angle sequence. To reduce autocorrelation and minimize data storage requirements, the time resolution of the radar data was reduced by using only the data volumes obtained at one-hour time intervals.

Radial velocity gates were automatically dealiased using a University of Washington algorithm. To both the radial velocity and reflectivity data, a digital terrain mask was applied to remove virtually all terrain clutter and shadowing in the radar volumes. The volumes were then reformatted and interpolated to a

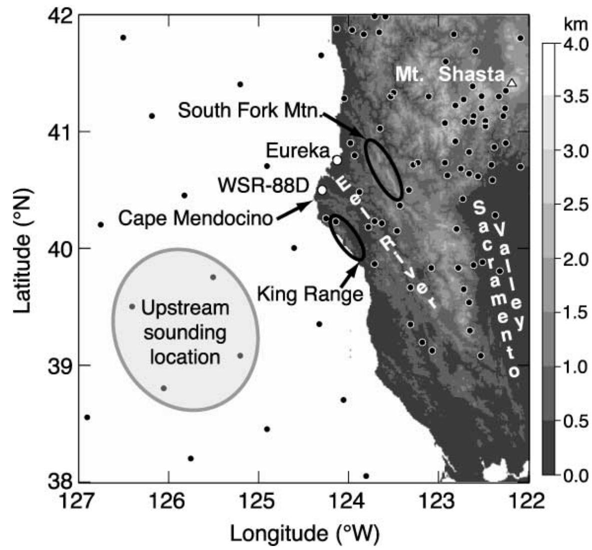

Figure 1. MAP of coastal Northern California, with terrain elevation (km above MSL) shaded. White circles over land represent automated rain-gauge stations; black dots over ocean depict the locations of Eta-model grid points. The four points enclosed by the ellipse were horizontally averaged to produce a synthetic sounding representative of the upstream flow. Important geographic features are labeled.

* *Corresponding author address:* Curtis N. James, Embry-Riddle Aeronautical Univ., Department of Meteorology, 3700 Willow Creek Road, Prescott, AZ 86301-3720; e-mail: Curtis.James@erau.edu.

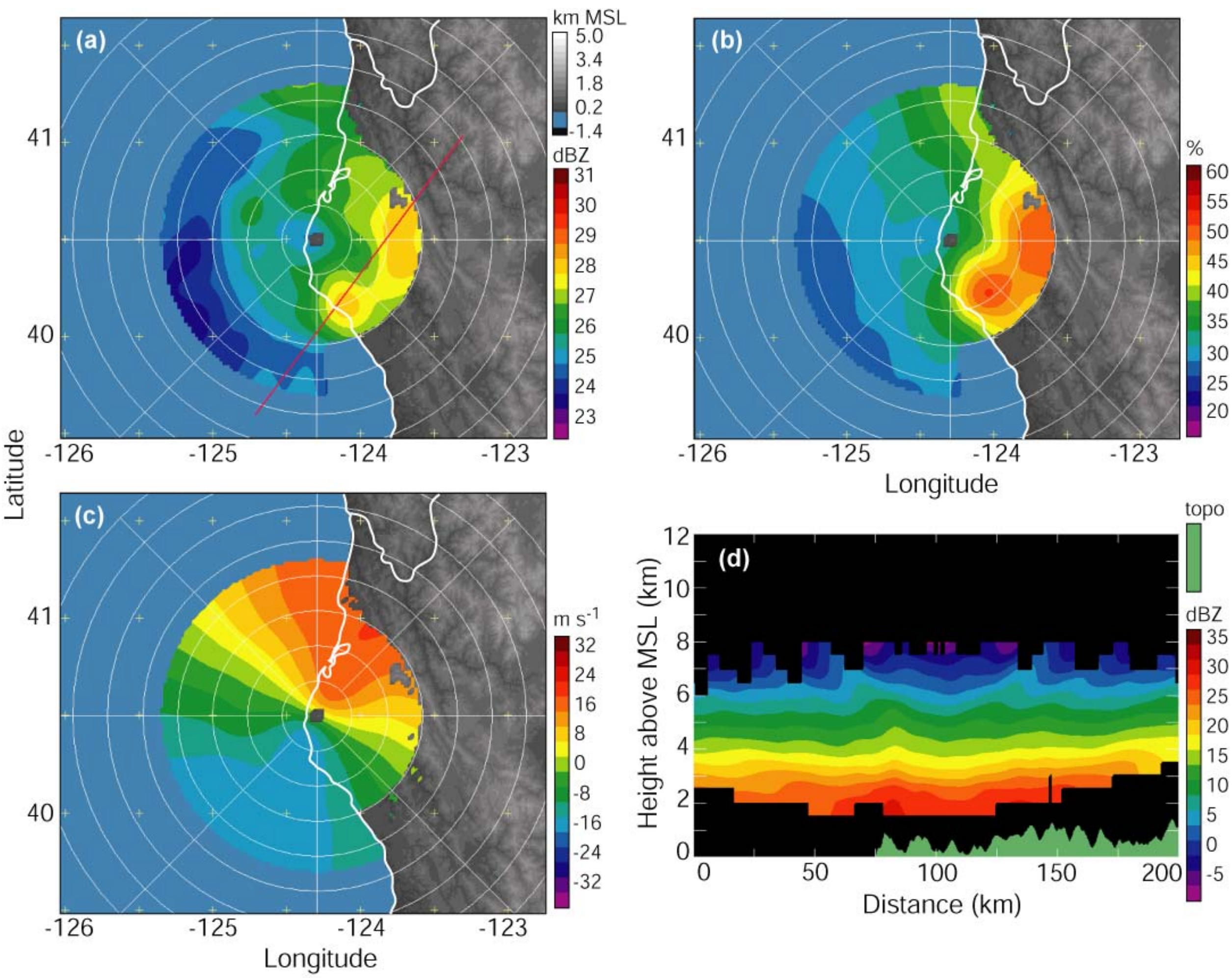

Figure 2. Eureka WSR-88D radar-derived precipitation climatology obtained for all heavy precipitation events. Constant altitude plots at an altitude of 2.0 km depict (a) mean reflectivity [dBZ], (b) the rainfall frequency, or percentage of radar volumes in which the reflectivity was at least 13 dBZ, and (c) mean Doppler radial velocity [m s^{-1}]. Negative (positive) radial velocity indicates flow towards (away from) the radar. Range ring spacing is 20 km, and azimuth lines are drawn every 45°. The thick white contour represents the coastline. In (d), a vertical cross-section plot of mean reflectivity [dBZ] is shown from southwest to northeast along the red line in (a), with the underlying terrain shaded green.

Cartesian grid of dimensions 2 km × 2 km × 0.5 km and displayed with terrain (after James et al. 2000).

Using the interpolated radar volumes, reflectivity and radial velocity means and superposed epoch analyses (e.g., Reed and Recker 1971) were computed following Houze et al. (2001). To reduce unwanted noise and radar artifacts, inverse range-squared horizontal smoothing was then applied at each interpolation grid point within a 16-km horizontal radius of influence for all horizontal maps (6-km horizontal radius for all vertical cross sections).

The superposed epoch analyses led to conclusions about the sensitivity of the precipitation in the vicinity of Eureka to dynamic and thermodynamic variables of the offshore flow. These upstream variables were estimated using analyses and 6-h forecasts from a 90-km Eta model grid. The model data at the four upstream model grid points bounded by the ellipse in Fig. 1 were horizontally averaged to produce smooth vertical soundings at 6-h intervals. Model grids were available for 1116 of the radar volumes.

The 900 – 800 mb layer (1 – 2 km MSL) in the synthetic soundings, corresponding to the low-level jet altitude, was used to estimate the static stability, wind speed, wind direction, and dew point temperature upwind. The static stability was represented by the moist Brunt-Väisälä frequency (Durran and Klemp 1982), and computed using finite differences. The 700 – 500 mb layer in the synthetic soundings was used to represent "mid-level" characteristics of the flow.

Averaged over all heavy rain events, these synthetic soundings indicated deep clockwise turning of the wind with height, suggesting the presence of warm advection and frictional turning at low levels.

Moist, conditionally unstable, unblocked flow was prevalent below 800 mb, with drier more stable air aloft. However, as will be shown below, the orographic precipitation varied dramatically depending on variations in the stability of the low-level (900 – 800 mb) flow impinging on the coastal mountains.

3. RADAR CLIMATOLOGY

Figure 2*a* shows the 2.0-km altitude horizontal display of reflectivity over Coastal Northern California, averaged over the 61 heavy precipitation days. Partial beam shadowing occurred behind South Fork Mountain (Fig. 1) and other terrain features, and corresponding radar gates beyond those obstacles to the beam were removed from the dataset. Removal of these blocked and partially blocked beams results in the circle of radar observations being much smaller to the east of the radar than to the west in Figs. 2a - c and 3a, c.

Despite the prevalence of unblocked flow during the heavy rain events, the overall pattern of reflectivity in Fig. 2a indicates upstream enhancement. The echo contours offshore are oriented roughly parallel to the coast, with echo intensity generally increasing towards shore. A quasi-circular maximum of reflectivity is apparent offshore at radar range of about 40 km in Fig. 2a. This curved maximum is mainly caused by bright-band patterns, associated with melting of ice particles. Over the terrain, especially on the windward side of the gradually upward sloping Coastal Range and over the smaller-scale peaks (i.e. King Range and South Fork Mountain; Fig. 1), greater reflectivity was observed.

Fig. 2b depicts the percentage of radar volumes in which the reflectivity equaled or exceeded 13 dBZ, which is roughly equivalent to a rainfall rate of 0.2 mm/h. Overall, the patterns in Fig. 2a and 2b are qualitatively similar, suggesting that orographic forcing primarily makes precipitation more *frequent* rather than more *intense*. Calculations of mean conditional rainfall rate (not shown), which is related to mean echo intensity, confirm this result, with the exception that slightly higher echo intensity occurred both over the higher terrain and offshore within roughly 60 km of the coast.

The prevailing Doppler velocity at 2.0 km MSL over all 1176 radar volumes (Fig. 2c) was nearly perpendicular to the Coastal Range from the southwest at speeds approaching 20 m s-1 at 2.0 km MSL. Maps of the Doppler velocities at other altitudes indicated the wind was veering with height, especially below 3-km MSL altitude, consistent with frictional turning and/or warm advection.

The vertical cross section of average reflectivity in Fig. 2d, taken parallel to the prevailing southwesterly wind along the red line in Fig. 2a, shows the vertical structure of the orographic precipitation. The portion of the cross section located within 45 km of the shore included echo within the layer 1-3 km MSL. However, the echo was truncated below this layer as a result of beam geometry. The strongest average reflectivity occurred over the first major peak of terrain (i.e. the King Range; located at about 70 km on the horizontal scale in Fig. 2d). This maximum extends to the upper levels as an upward bending of the reflectivity contours over the first peak. This behavior was evident in Houze et al. (2001) and by Medina and Houze (2003) over the Mediterranean side of the Alps amid unblocked flow.

In contrast to the sounding and radar data just discussed, the upstream enhancement far ahead of the first peak of terrain is suggestive of blocking. The climatological radar echo pattern in the Eureka radar is thus a combination of unblocked and blocked characteristics. Since the radar data for the major rain events considered here do not extend below the 1-km level (nor below 3 km far from the radar), it is impossible to know the reflectivity or radial velocity conditions in the boundary layer or near the sea surface. It is possible that some of the echo enhancement seen in the echo climatology over the ocean upstream from the coastal mountains could have been influenced by a very thin layer of near-surface air, in contact with the cold ocean, blocked and dammed against the coastal terrain. Further evidence is needed to confirm this suspicion. Neiman et al. (2004) have found such a thin layer off the coast of California and have suggested that its blocking modifies landfalling cyclones with low-level jets of the type considered here. The air above the surface layer could have been lifted over this shallow layer of cold air enough to produce the offshore upstream enhancement. The layer lifted above the thin layer of marine air could have then proceeded over the coastal mountains in a relatively unblocked fashion. This behavior might help explain why upstream enhancement (normally associated with blocked flow) occurs offshore in an otherwise relatively unblocked flow (Medina and Houze 2003). The shallow blocked pool of cold marine air might work together with the stability of the cross-barrier flow above the shallow surface layer to explain the echo enhancement upstream of the mountains.

4. RELATIONSHIP OF RADAR CLIMATOLOGY TO MID-LEVEL FLOW

A number of superposed epoch analyses were performed on the radar data to provide insight into the sensitivity of heavy coastal precipitation to characteristics of the low-level (900 – 800 mb) and mid-level (700 – 500 mb) flow. Of these analyses, most are not presented here. However, results of these analyses indicate that precipitation was dramatically greater and more widespread when the mid-level (700 – 500 mb) flow was stronger and more humid. The stronger mid-level flow is an indication of the strength of the synoptic forcing and the tendency for hydrometeors to spread over a greater horizontal distance before falling to the ground.

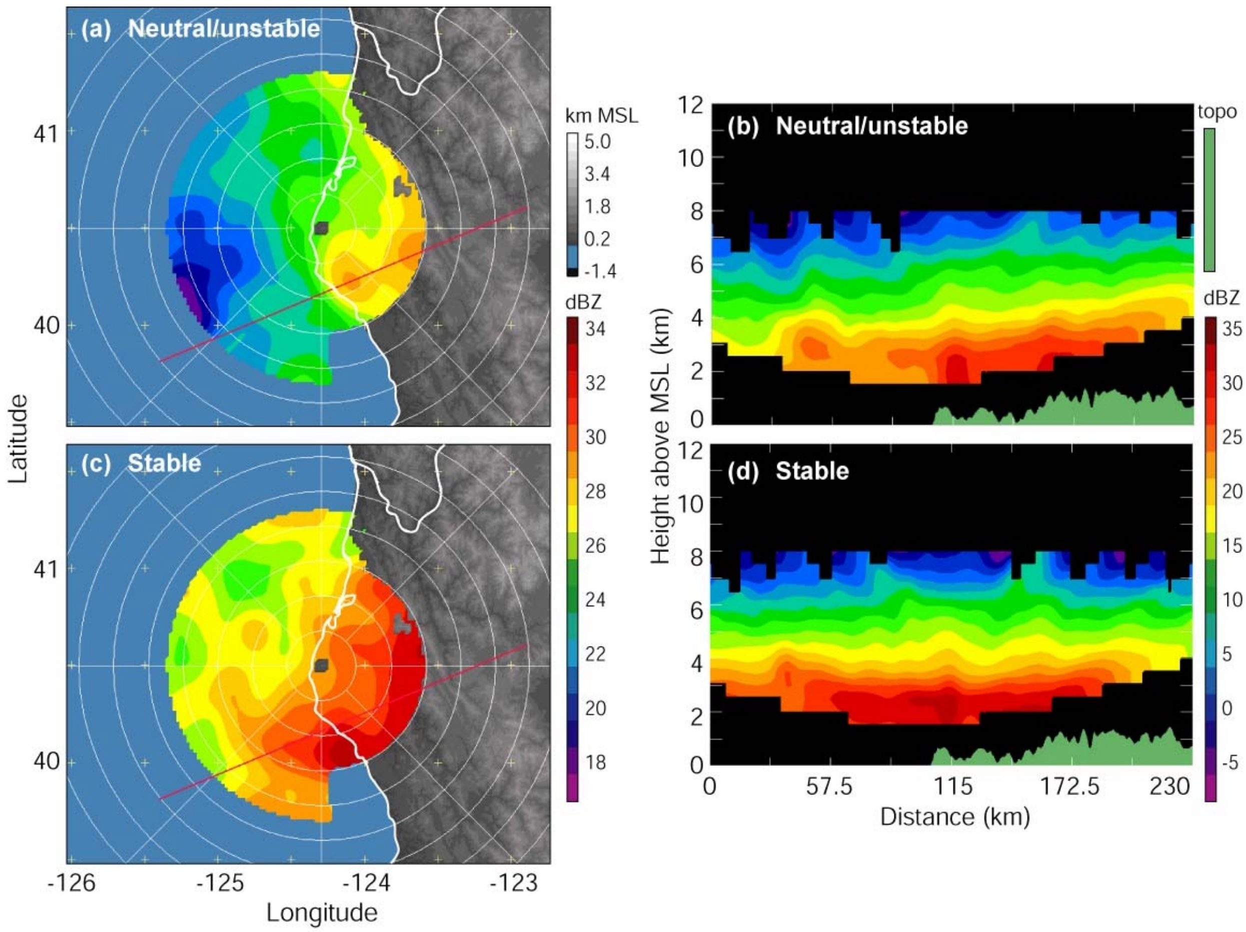

Figure 3. Of those hourly radar volumes whose 900 – 800 mb wind direction was west-southwesterly (between 225 and 270° azimuth) and the 0°C level was at least 2.5 km MSL, this analysis depicts the mean reflectivity [dBZ] at 2.0 km altitude during heavy rain events when the layer-averaged 900 – 800 mb Brunt-Väisälä frequency was (a) zero or imaginary and (c) greater than zero. Vertical cross-section plots from west-southwest to east-northeast along the red segments (a) and (c) are shown in (b) and (d) respectively, with the underlying terrain shaded green.

5. SENSITIVITY OF PRECIPITATION TO LOW-LEVEL FLOW CHARACTERISTICS

Superposed epoch analyses based on low-level (900 – 800 mb) wind direction (not shown) indicate that south-southwesterly and southwesterly flow, which was most likely pre-frontal or frontal, produced greater precipitation over the entire domain of the Eureka radar. This flow apparently brought plentiful moisture into the region, and typically possessed a higher static stability. Flow of this direction also evidently experienced the greatest mechanical lifting relative to the northwest-to-southeast oriented terrain in northern California. Flow of a more westerly or northwesterly direction was likely post-frontal and more intermittent and convective in nature, producing less rainfall.

Analyses of low-level wind speed (not shown) reveal that the overall response of the reflectivity was less and more concentrated over the mountains when the wind was weaker. Stronger flow produced a stronger response, with greater downwind spillover of precipitation.

Of particular note, low-level static stability was strongly associated with rainfall. Figure 3 divides the west-southwesterly low-level flow events with the 0°C level ≥ 2.5 km MSL into unstable/neutral and stable categories. Figures 3a and 3b show the unstable/neutral cases defined as those for which the moist Brunt-Väisälä frequency was imaginary or zero. Figures 3c and 3d show the stable cases for which the moist Brunt-Väisälä frequency was greater than zero.

Figure 3 illustrates that the reflectivity was stronger everywhere when absolute stability prevailed. In particular, upstream enhancement was much stronger under stable conditions. During stable events, the leading edge of the upstream enhancement was marked by a strong gradient of reflectivity. In both vertical cross sections, the leading edge of the offshore enhancement (at about 50 km on the horizontal scale) is marked by an echo maximum and upward protuberance of the reflectivity contours, similar to that seen near the first peak of terrain onshore. While the intensity and upstream extent of this echo structure may be exaggerated by bright band influences, it suggests the southwesterly flow was responding to an offshore cold pool similar to the way it responded to the terrain proper.

The offshore precipitation between the initial reflectivity core offshore and the first peak of terrain, and between the first and second peaks of terrain, exhibited a stratiform vertical structure with a bright band under both unstable/neutral (Fig. 3b) and stable (Fig. 3d) conditions. These observations indicate that the coastal terrain, and possible offshore cold pools, were enhancing the basic stratiform precipitation structure of the landfalling baroclinic storm systems, and that this overall enhancement was punctuated by sudden upward responses of the unblocked low-level flow, first to the leading edge of an offshore near-surface cold pool, then to the first and second major rises of terrain.

6. SUMMARY

Major rain events in northern California occurred during southwesterly flow characterized by a low-level jet and a high influx of tropical moisture. South and east of Eureka, the southwesterly low-level flow was perpendicular to a series of two-dimensional mountain ridges. Orographic enhancement of the precipitation occurred both over the coastal mountain ranges and upstream over the ocean. However, the impinging flow (above the 1-km level) was strong enough to be unblocked by the terrain, and the occurrence of upstream enhancement was in this respect unexpected. It is possible that a thin layer of cold marine air (<1 km deep) was dammed against the coastal mountains, and the unblocked flow lifting over the cold pool was enough to produce upstream enhancement.

Vertical cross sections through the climatological echo pattern of the heavy rain events were generally stratiform in character from over the ocean to inland over the mountains. Directly over the mountains, the broad pattern of the mean reflectivity field on the scale of the overall region of coastal mountains showed upward sloping echo contours indicative of a general upslope orographic enhancement. This basic stratiform echo pattern over the mountains was interrupted by an embedded core of maximum mean reflectivity over the first major peak of terrain encountered by the unblocked flow. This core was the strongest feature of the orographic precipitation pattern. A secondary echo core occurred over the second major peak of the coastal mountain terrain. It was similar to the core over the first peak of terrain, but not as intense.

The orographically enhanced precipitation and associated upstream, offshore, enhanced precipitation were stronger when the upstream flow was stronger or when the lower atmosphere was statically stable as opposed to neutral or slightly conditionally unstable. Stable conditions may conform the flow and associated precipitation more tightly to the topography. The slight instability in some cases may have produced somewhat more random patterns, less coherent to the topography.

7. REFERENCES

Durran, D. R., and J. B. Klemp, 1982: On the effects of moisture on the Brunt-Väisälä frequency. *J. Atmos. Sci.,* **39,** 2152-2158.

Houze, R. A., Jr., C. N. James, and S. Medina, 2001: Radar observations of precipitation and airflow on the Mediterranean side of the Alps: Autumn 1998 and 1999. *Quart. J. Roy. Meteor. Soc.,* **127,** 2537-2558.

James, C. N., S. R. Brodzik, H. Edmon, R. A. Houze, Jr., and S. E. Yuter, 2000: Radar data processing and visualization over complex terrain. *Wea. Forecasting,* **15,** 327-338.

Medina, S., and R. A. Houze, Jr., 2003: Air motions and precipitation growth in Alpine storms. *Quart. J. Roy. Meteor. Soc.,* special MAP issue, **129,** 345-371.

Neiman, P. J., P. O. G. Persson, F. M. Ralph, D. P. Jorgensen, A. B. White, and D. E. Kingsmill, 2004: Modification of fronts and precipitation by coastal blocking during an intense landfalling winter storm in southern California: Observations during CALJET. *Mon. Wea. Rev.,* **130,** 1468-1492.

Reed, R. J., and E. E. Recker, 1971: Structure and properties of synoptic-scale wave disturbances in the equatorial western Pacific. *J. Atmos. Sci.,* **28,** 1117-1133.